
Neural Rendering 3D

Johnny Núñez, Marcos Plaza, Qijun Jin

Department of Computer Science
University of Barcelona
mat.ub.edu

Abstract

1 The term Neural Volume Rendering refers to a method that generates imagery or
2 video by tracing the path of a ray in a neural network scene, following the path of
3 the ray, and taking an integral during the ray at some time in the future. Typically, a
4 neural network such as this one would be used if, for example, the rays are encoded
5 by a multilayer perceptron, which encodes quantities associated with the rays such
6 as density and color, which in turn are combined to generate an image. Therefore,
7 in this paper, we explain different neural networks to explain the rendering 2D to
8 3D.

9 **Keywords:** Neural Rendering, Geometric Deep Learning, NeRF

10

1 Introduction

11 Is it possible to render a 3D object from 2D images and save a lot of time and money with sensors and
12 another kind of hardware? Is it possible to create objects automatically without having to create them
13 manually in graphics engines such as Unreal Engine [1] or other softwares? And if it kept the lighting
14 and shadows of the photograph, is it possible? Many of the problems encountered daily when making
15 movies, real-time rendering, or video games are the cost of implementing such rendering, either with
16 sensory suits for humans, cameras with multiview photography such as Panoptic [2]. To translate the
17 accuracy of the real world to the virtual world requires mechanisms that are fast and inexpensive,
18 where the creation of the new metaverse is rapidly growing thanks to realistic and complex virtual
19 worlds.

20 These problems lead us to think about the existence of models that can generate hyper-realistic
21 renderings in real time from a set of images or even a single image. To address this problem, what
22 is called Geometric Deep Learning [3] (Johnny, Jin, Marcos) was defined, not only to generate 3D
23 renderings but also to learn about multidimensional data and extract relevant information.

24 Geometric Deep Learning in Computer Vision is a new field of machine learning that can learn from
25 complex data such as graphs, images, and multidimensional points. It is an attempt at geometric
26 unification of a broad class of machine learning problems from the perspectives of symmetry and
27 invariance. It seeks to apply traditional neural networks to 3D objects, graphs, and varieties. In our
28 case, it is a specific problem, a neural network is applied to multi 2D images to create 3D objects.

29 The algorithms that appear in this article cannot be explained without first learning about some of the
30 real-time rendering techniques of recent years. These technologies make it possible to generate or
31 calculate images (in two dimensions) from a 2D or 3D model. One of the best known is raytracing
32 [4] (Marcos), based on emulating the physical behaviour of light on landscape elements, by using the
33 concept of rays. Roughly speaking, these rays will be projected into the scene and will be bounced

34 back and forth a number of times to finally decide what colour to paint the pixel. Another technique
 35 used in computer graphics is known as Volume Ray Marching or Volume Ray Casting. This method
 36 processes volume data and must not be mistaken with ray casting in the sense used in ray tracing,
 37 which processes surface data. In the volumetric variant, the computation does not stop at the surface
 38 but "pushes through" the object, sampling the object along the ray. Therefore, here is an image to
 39 compare both technologies.

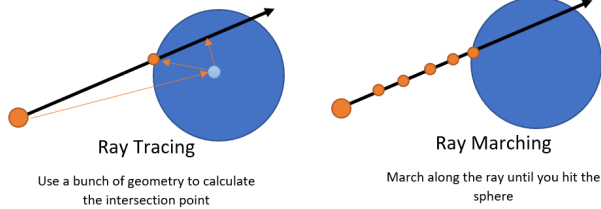


Figure 1: Ray Tracing versus Ray Marching

40 Given a 3D model, the task of this Volume Ray Casting algorithm [5] (Marcos) is to approximate for
 41 each ray which colour each voxel (each cell in three-dimensional space) should be painted in. How is
 42 this done? Without going too deep, we will do it through the so-called transfer function ($f(x)$). As we
 43 have said, this function takes the numerical data from the dataset to decide what colour and opacity
 44 pixels should be painted. Thus, by manipulating this function $f(x)$ we are changing the display of
 45 the objects in the scene. Therefore, with this function we can compute the pixel's color along all
 46 rays. In essence, this function for mapping the colour of every coordinate in the image, called transfer
 47 function $f(x)$ will be the one used by the algorithms explained in this paper. Therefore, that given a
 48 new angle or a new observer position, we will be generating a new and accurate visualization simply
 49 by predicting every value for every pixel.

50 2 State of the Art

51 The focus of this section is to introduce Neural Rendering and its development, as well as the NeRF
 52 algorithms and how they are derived.

53 2.1 Background

54 First of all, these occupancy networks [6] (Jin) are based on implicit, coordinate-based learning of
 55 occupancy. Based on a feature vector and a 3D point, a network of five ResNet blocks predicts
 56 binary occupancy. Similarly exists a 6 layer MLP decoder that is used in IM-NET [7] (Marcos) to
 57 predict binary occupancy given a feature vector and a 3D coordinate. This algorithm can be used
 58 for auto-encoding, shape generation (GAN-style), and single-view reconstruction. DeepSDF [8]
 59 (Johnny) is another method for regressing a signed distance function directly from a 3D coordinate,
 60 as well as a latent code. There is an 8-layer MLP with skip connections at layer 4, setting a trend.
 61 Finally, PIFu [9] (Marcos) demonstrates that it is possible to learn highly detailed implicit models by
 62 reprojecting 3D points into pixel-aligned feature representations. This idea will later be reprised to
 63 great effect in PixelNeRF.

64 On the other hand, several other approaches are built on top of the implicit function concept. First,
 65 Structured Implicit Functions [10] (Johnny) show that you can combine these implicit representations,
 66 e.g., simply by summing them. CVxNet [11] (Jin) takes a pointwise max (in 3D) to combine signed
 67 distance functions. Additionally, the paper contains several other elegant methods for reconstructing
 68 an object from depth or RGB images. Similarly exists BSP-Net [12] (Johnny) which is in many
 69 ways like CvxFNet, but it relies on binary space partitioning at its core to generate polygonal meshes
 70 natively, rather than by using expensive meshing methods. To represent larger, extended scenes,
 71 Deep Local Shapes [13] (Jin) store a DeepSDF latent code in a voxel grid. Scene Representation

72 Networks [14] (Marcos) or SRN are quite similar to DeepSDF in terms of architecture, but include a
 73 differentiable ray marching algorithm for determining the closest point of intersection of an implicit
 74 surface and an MLP which regresses color, enabling it to be learned from multiple posed images.
 75 Differentiable Volumetric Rendering [15] (Marcos) shows that implicit scene representations can
 76 be paired with a differentiable renderer, making the system trainable from images, similar to SRN.
 77 Despite the use of the term volumetric renderer, the core contribution is a clever trick to make depth
 78 of the implicit surface differentiable: no volume integration is required. It has a more sophisticated
 79 surface light field representation and can also refine camera pose learning. Implicit Differentiable
 80 Renderer [16] (Marcos) presents a similar technique. The neural articulated shape approximation
 81 [17] (Jin) comprises implicit functions to represent articulated objects such as human bodies.

82 **2.2 NeRF Models**

83 In the NeRF [18] (Johnny, Jin, Marcos), they use the DeepSDF architecture, but the regression is not
 84 based on a signed distance function, but density and color. In the next step, a numerical integration
 85 method (which is easily differentiable) is used to approximate the true volumetric rendering step.
 86 NERF++[19] (Jin) proposes a separate NeRF model for handling unbounded scenes in the background.
 87 The Nerfies[20] (Johnny) model and its underlying D-NeRF model use a second MLP to apply a
 88 deformation to each frame of the video. D-NeRF [21] (Johnny), based on the same acronym, is
 89 quite similar to Nerfies. However, it is limited only to translations. Neutral Reflectance Fields [22]
 90 (Marcos) extend NeRF by adding a local reflection model in addition to density. The relighting
 91 results are impressive, albeit with a single point source. As a conditional variant of NeRF, GRAF [23]
 92 (Johnny), "Generative Model for Radiance Fields" is able to add both appearance and shape latent
 93 codes, while viewpoint invariance is achieved through the use of GAN-style training. Neural Scene
 94 Graphs [24] (Jin) integrate several object-centric NeRF models into a scene graph. A NeRF MLP is
 95 used in a pose estimation framework in NeRF [25] (Marcos). The fine-tuning of the poses can even
 96 improve view synthesis on standard datasets. However, illumination has not yet been addressed.

97 **3 Methodologies**

98 The scene reconstruction based on neural radiance field consists of 3 phases: Firstly, we need to define
 99 a set of 3D points for the camera in the scene. Then, using these 3D points with their corresponding
 100 viewing cones to train the neural network to generate the RGB color and its volume density. Finally,
 101 the 2D image is reconstructed by using a volume rendering to accumulate both RGB color and
 102 density.

103 By combining those output images, it can give us an impression of a real 3D scene which can be seen
 104 from different views.

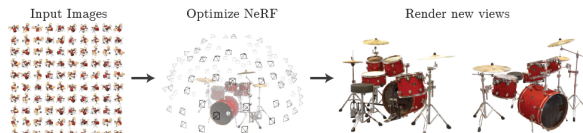


Figure 2: Reconstruction phases with NeRF

105 **3.1 Pipeline**

106 To know how the neural radiance field works, we have to explain the primitive data that involves in
 107 the neural network and then look in detail how is the training process.

108 For the input, we need two elements apart from the image itself: the 3D coordinates (x, y, z) at which
 109 it will perform the volume ray marching, and the direction (θ, ϕ) of the viewpoint at which we are
 110 looking for. These 5 primitive data are composed to be the continuous 5D scene representation, and

111 by optimizing these parameters in the neural network process, one can minimize the pixel-level color
 112 error between the generated set of images and the original ones.

113 The output of this neural network is the radiance emitted from every 3D point and viewpoint in the
 114 3D space with a volume density. The radiance emitted is the RGB color composition of the image,
 115 which is view-dependent, as the color representation viewed changes from a different viewpoint. The
 116 volume density, which is defined for every 3D point, is used to control the radiance saturation on the
 117 volume ray marching.

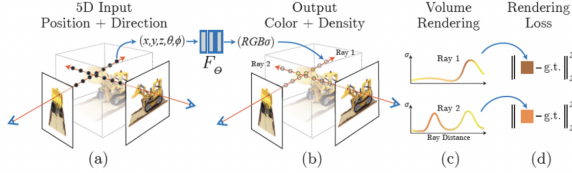


Figure 3: NeRF architecture

118 Based on the idea that our process is differentiable, the gradient descent method is applied to optimize
 119 the model by iteratively minimizing the error between the original image and the rendered image.
 120 Since this error is minimized from several viewpoints, the neural network is capable to train a model
 121 on a the set of original images, giving both accurate color and density to render.

122 3.2 Volume rendering

123 Volume rendering is a set of techniques used to display 2D projections of 3D discretely sampled data
 124 sets (usually 3D scalar fields). As seen on the introduction section, particularly on NeRF models,
 125 we are using the function known as transfer function $f(x)$, applied in the Volume Ray Marching
 126 algorithm. As previously mentioned, it takes a vector with the coordinates, density and angle to
 127 finally put a color and opacity in each pixel. The parameters of this function will be fitted by the
 128 Neural Network on it's training phase, so that predict the unknown values from a different point of
 129 view.

130 Here, the volume density is defined as the differential probability of a ray terminating at an in-
 131 finitesimal particle at a location x . Then the color expected $C(r)$ of camera ray is determined by
 132 $r(t) = o + td$ in between the near bound t_n and far bound t_f .

$$C(\mathbf{r}) = \int_{t_n}^{t_f} T(t) \sigma(\mathbf{r}(t)) \mathbf{c}(\mathbf{r}(t), \mathbf{d}) dt$$

133 where $T(t) = \exp\left(-\int_{t_n}^t \sigma(\mathbf{r}(s)) ds\right)$

134 The function $T(t)$ is the accumulated transmittance along the ray from t_n to t , which is computed as
 135 the probability that the ray travels from t_n to t without hitting any other object. Finally, to render a
 136 view given a virtual camera is to estimate the integral $C(r)$ of the continuous neural radiance field.

$$\hat{C}(\mathbf{r}) = \sum_{i=1}^N T_i (1 - \exp(-\sigma_i \delta_i)) \mathbf{c}_i$$

137 where $T_i = \exp\left(-\sum_{j=1}^{i-1} \sigma_j \delta_j\right)$ and $\delta_i = t_{i+1} - t_i$ is the distance between adjacent samples.
 138 Therefore, the alpha values is $\alpha_i = 1 - \exp(-\sigma_i \delta_i)$ for the alpha composition.

139 **3.3 Enhancement**

140 Actually, the basic implementation cannot generate high resolution render for a complex scene
 141 because of the low dimensional feature space. However, we can recover the idea of waves in the
 142 physics world, allowing us to enlarge the feature space by representing them in a frequency function.
 143 This data transformation is called **positional encoding**. Besides, another improvement technique
 144 based on the idea of increasing computational efficiency is the **hierarchical procedure**, which allow
 145 us to sample the N query points of the ray on demand.

146 **3.3.1 Positional encoding**

147 The positional encoding has emerged due to the fact that deep networks are biased towards learning
 148 low frequency functions. For a complex scene, it requires the network to compute a high-frequency
 149 variation in color and geometry, therefore the input data should be mapped into a higher dimensional
 150 space to preserve this high-frequency variation. The linear mapping γ changes our input dimension
 151 from \mathbb{R} to \mathbb{R}^{2L} .

$$\gamma(p) = (\sin(2^0\pi p), \cos(2^0\pi p), \dots, \sin(2^{L-1}\pi p), \cos(2^{L-1}\pi p))$$

152 Being L parameter to determine the frequency. This function is applied to both 3D points and the
 153 viewing cone, which are normalized in the range [-1, 1].

154 **3.3.2 Hierarchical sampling**

155 The algorithm samples each camera ray as a query of N equal distance points and the evaluation
 156 of neural radiance field network on these points is inefficient due to the radiance field presents free
 157 space and occlusion which does not provide any information on the rendered image. Therefore, the
 158 process to train the network must be selectively. Regarding to this, we need to optimize two networks
 159 at different levels of fineness: the coarse level and the fine level.

Firstly, we sample a set of N_c locations to determine the coarse network. Given the output of the
 coarse network, we apply a weighted sum to all sampled colors c_i along the ray. Then by normalizing
 the weights as:

$$\hat{w}_i = w_i / \sum_{j=1}^{N_c} w_j$$

160 it produces a piecewise constant probability density function along the ray.

161 The fine level is applied over the coarse level, yet again it has to sample a set of N_f locations to a
 162 certain subsets of coarse level and then the color rendered of the ray is computed taking into account
 163 the union of both samples $N_c + N_f$. On this fine level, the model is able to allocate more samples to
 164 regions that contain visible content.

165 Considering these enhancements over the basic implementation, at each optimization iteration, the
 166 batch of camera rays which is randomly sampled will be processed with the hierarchical sampling
 167 to query 2 types of samples: N_c samples from the coarse network and $N_c + N_f$ samples from the
 168 fine network. Then the volume rendering will proceed to render a color of each ray from both sets of
 169 samples. Indeed, the loss function has to be adapted taking into account both set of renders.

$$\mathcal{L} = \sum_{\mathbf{r} \in \mathcal{R}} \left[\left\| \hat{C}_c(\mathbf{r}) - C(\mathbf{r}) \right\|_2^2 + \left\| \hat{C}_f(\mathbf{r}) - C(\mathbf{r}) \right\|_2^2 \right]$$

170 where \mathcal{R} is the set of rays in each batch, $C(r)$ is the true pixel color, $\hat{C}_c(r)$ is the coarse level
 171 predicted pixel color and $\hat{C}_f(r)$ is the fine level predicted pixel color for ray r .

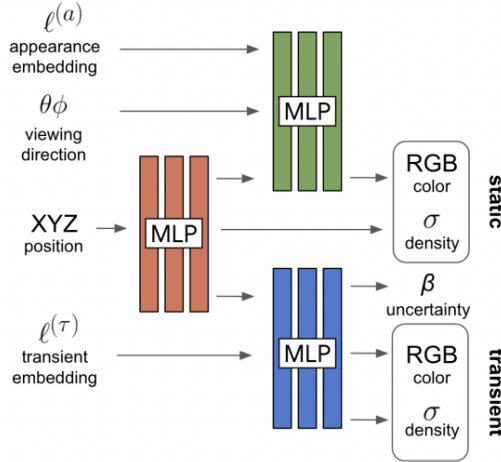


Figure 4: Multimodal embedding in NeRF-W, Image from Original Paper

173 As part of a low-dimensional latent embedding space, NeRF-W [26] (Johnny, Jin, Marcos) captures
 174 the lighting and photometric postprocessing. It is possible to smoothen out the variation in appearance
 175 by interpolating between two embeddings without affecting the 3D geometry of the object. A major
 176 difference with NeRF is the oriented and photometric postprocessing in the form of a low-dimensional
 177 latent embedding space. There is no lighting nor shading information in the vertex data of a mesh,
 178 but it smooths out the variations as a result. A smooth interpolation between two embeddings allows
 179 you to capture the variation in appearance without altering the geometry of the 3D object. An
 180 orientation and photometric postprocessing method in a low-dimensional embedding space using
 181 a latent embedding function. We perform the inverse lighting and photometry in the latent space,
 182 without having to touch the vertex data. Whenever a photographer takes a series of images, we can
 183 be used to compute the following information: orientation of the camera (rotation, 3-D translation),
 184 position of the light sources around the scene (3-D translation), photometric correction of the images
 185 (relative intensity of each pixel in each image) is particularly useful when capturing photos of static
 186 scenes or when giving a consistent rendering of the scene.

187 4 Results and Discussion

188 In this section, we present the metrics that use Nerf and his derivations. - Evaluation Metric

- 189 • PSNR(Peak Signal-to-Noise Ratio): higher PSNR, lower MSE. Lower MSE implies less
 190 difference between the ground truth image and the rendered image. Thus, the higher PSNR,
 191 the better model.
- 192 • SSIM(Structural Similarity Index): Checks the structural similarity with the ground truth
 193 image model. The higher SSIM, the better model.
- 194 • LPIPS(Learned Perceptual Image Patch Similarity): Determines the similarity with the view
 195 of perception; using VGGNet. The lower LPIPS, the better model.

196 The results obtained are promising. The Neural Radiance Field model weighs only 5Mb. Neural
 197 Radiance Field is capable of producing high-quality images and videos, even in real time. The model
 198 is easy to train and does not suffer from overfitting. It can be used for the generation of realistic
 199 images and videos for a variety of applications.



Figure 5: Result NeRF

200 The next step will be to try to improve the model even further. The current model is not capable
 201 of generating all types of images. For example, it is not capable of generating images of faces or
 202 of realistic textures. The most important direction for further research is to make the model more
 203 light-weight and to increase its real-time capabilities that already exist in models such as NeRF++.



Figure 6: Result NeRF 3D

204 On the other hand, NeRF-W can reconstruct monuments in 3D. This would be very useful to make
 205 hyper-realistic maps of buildings with images from the internet, no matter the people or objects that
 206 are moving at that moment if we have a large enough dataset.



Figure 7: Result NeRF-W

207 5 Conclusion

208 The Neural Radiance Fields seems to us just the beginning of the new reconstruction technique to
 209 come out in the market. The benefit of this methods is that the scene reconstructed occupies even less
 210 than the single image processed to the input. So there is a big improvement in memory usage in order
 211 to compute a new render in a scene.

212 However, this technique takes within 1 or 2 day to learn all the weights required, which is a lot of time
 213 to speed for giving the scene, even though by using more GPU will decrease the computational time.
 214 Another counterpart of Neural Radiance Fields is that the object is reconstructed by a set of weights
 215 beyond a 3D space (scene) taken a set of the images and the corresponding viewpoints, meaning that
 216 the creation does not preserves the 3D coordinates of the object in comparison with this traditional
 217 technique of rendering.

218 To conclude, will NeRF technology be applied in the future on real-time graphics? Clearly we have
 219 no answer to this question. From the most objective point of view possible, the computer graphics
 220 industry is a very mature and established sector that has seen many advances in both hardware and

221 software. By means of polygons and meshes, as well as raytracing algorithms among many other
222 technologies, and the actual results obtained is quite awesome. But it is conceivable that in the not
223 too distant future, mixed computer graphics generation techniques will be applied in which machine
224 learning, in this case Neural Radiance Fields, will play an important role.

225 **References**

- 226 [1] Epic Games. Unreal engine, 2022.
- 227 [2] Hanbyul Joo, Tomas Simon, Xulong Li, Hao Liu, Lei Tan, Lin Gui, Sean Banerjee, Timo-
228 thy Scott Godisart, Bart Nabbe, Iain Matthews, Takeo Kanade, Shohei Nobuhara, and Yaser
229 Sheikh. Panoptic studio: A massively multiview system for social interaction capture. *IEEE*
230 *Transactions on Pattern Analysis and Machine Intelligence*, 2017.
- 231 [3] Michael M. Bronstein, Joan Bruna, Taco Cohen, and Petar Veličković. Geometric deep
232 learning: Grids, groups, graphs, geodesics, and gauges. *ArXiv*, abs/2104.13478, 2021.
- 233 [4] Andrew S Glassner. *An introduction to ray tracing*. Morgan Kaufmann, 1989.
- 234 [5] Kun Zhou, Zhong Ren, Stephen Lin, Hujun Bao, Baining Guo, and Heung-Yeung Shum. Real-
235 time smoke rendering using compensated ray marching. In *ACM SIGGRAPH 2008 papers*,
236 pages 1–12. 2008.
- 237 [6] Lars M. Mescheder, Michael Oechsle, Michael Niemeyer, Sebastian Nowozin, and Andreas
238 Geiger. Occupancy networks: Learning 3d reconstruction in function space. *2019 IEEE/CVF*
239 *Conference on Computer Vision and Pattern Recognition (CVPR)*, pages 4455–4465, 2019.
- 240 [7] Zhiqin Chen and Hao Zhang. Learning implicit fields for generative shape modeling. *2019*
241 *IEEE/CVF Conference on Computer Vision and Pattern Recognition (CVPR)*, pages 5932–5941,
242 2019.
- 243 [8] Jeong Joon Park, Peter R. Florence, Julian Straub, Richard A. Newcombe, and S. Love-
244 grove. Deepsdf: Learning continuous signed distance functions for shape representation. *2019*
245 *IEEE/CVF Conference on Computer Vision and Pattern Recognition (CVPR)*, pages 165–174,
246 2019.
- 247 [9] Shunsuke Saito, Zeng Huang, Ryota Natsume, Shigeo Morishima, Angjoo Kanazawa, and Hao
248 Li. Pifu: Pixel-aligned implicit function for high-resolution clothed human digitization. *2019*
249 *IEEE/CVF International Conference on Computer Vision (ICCV)*, pages 2304–2314, 2019.
- 250 [10] Kyle Genova, Forrester Cole, Daniel Vlasic, Aaron Sarna, William T. Freeman, and Thomas A.
251 Funkhouser. Learning shape templates with structured implicit functions. *2019 IEEE/CVF*
252 *International Conference on Computer Vision (ICCV)*, pages 7153–7163, 2019.
- 253 [11] Boyang Deng, Kyle Genova, Soroosh Yazdani, Sofien Bouaziz, Geoffrey E. Hinton, and Andrea
254 Tagliasacchi. Cvxnet: Learnable convex decomposition. *2020 IEEE/CVF Conference on*
255 *Computer Vision and Pattern Recognition (CVPR)*, pages 31–41, 2020.
- 256 [12] Zhiqin Chen, Andrea Tagliasacchi, and Hao Zhang. Bsp-net: Generating compact meshes
257 via binary space partitioning. *2020 IEEE/CVF Conference on Computer Vision and Pattern*
258 *Recognition (CVPR)*, pages 42–51, 2020.
- 259 [13] Rohan Chabra, Jan Eric Lenssen, Eddy Ilg, Tanner Schmidt, Julian Straub, S. Lovegrove,
260 and Richard A. Newcombe. Deep local shapes: Learning local sdf priors for detailed 3d
261 reconstruction. In *ECCV*, 2020.
- 262 [14] Vincent Sitzmann, Michael Zollhoefer, and Gordon Wetzstein. Scene representation networks:
263 Continuous 3d-structure-aware neural scene representations. *ArXiv*, abs/1906.01618, 2019.

- 264 [15] Michael Niemeyer, Lars M. Mescheder, Michael Oechsle, and Andreas Geiger. Differentiable
265 volumetric rendering: Learning implicit 3d representations without 3d supervision. *2020
266 IEEE/CVF Conference on Computer Vision and Pattern Recognition (CVPR)*, pages 3501–3512,
267 2020.
- 268 [16] Lior Yariv, Yoni Kasten, Dror Moran, Meirav Galun, Matan Atzmon, Ronen Basri, and Yaron
269 Lipman. Multiview neural surface reconstruction by disentangling geometry and appearance.
270 *arXiv: Computer Vision and Pattern Recognition*, 2020.
- 271 [17] Timothy Jeruzalski, Boyang Deng, Mohammad Norouzi, J. P. Lewis, Geo rey E. Hinton, and
272 Andrea Tagliasacchi. Nasa: Neural articulated shape approximation. *ArXiv*, abs/1912.03207,
273 2020.
- 274 [18] Ben Mildenhall, Pratul P. Srinivasan, Matthew Tancik, Jonathan T. Barron, Ravi Ramamoorthi,
275 and Ren Ng. Nerf: Representing scenes as neural radiance fields for view synthesis. In *ECCV*,
276 2020.
- 277 [19] Kai Zhang, Gernot Riegler, Noah Snavely, and Vladlen Koltun. Nerf++: Analyzing and
278 improving neural radiance fields. *ArXiv*, abs/2010.07492, 2020.
- 279 [20] Keunhong Park, U. Sinha, Jonathan T. Barron, Sofien Bouaziz, Dan B. Goldman, Steven M.
280 Seitz, and Ricardo Martin-Brualla. Nerfies: Deformable neural radiance fields. 2020.
- 281 [21] Albert Pumarola, Enric Corona, Gerard Pons-Moll, and Francesc Moreno-Noguer. D-nerf:
282 Neural radiance fields for dynamic scenes. *2021 IEEE/CVF Conference on Computer Vision
283 and Pattern Recognition (CVPR)*, pages 10313–10322, 2021.
- 284 [22] Sai Bi, Zexiang Xu, Pratul P. Srinivasan, Ben Mildenhall, Kalyan Sunkavalli, Milovs Havsan,
285 Yannick Hold-Geoffroy, David J. Kriegman, and Ravi Ramamoorthi. Neural reflectance fields
286 for appearance acquisition. *ArXiv*, abs/2008.03824, 2020.
- 287 [23] Katja Schwarz, Yiyi Liao, Michael Niemeyer, and Andreas Geiger. Graf: Generative radiance
288 fields for 3d-aware image synthesis. *ArXiv*, abs/2007.02442, 2020.
- 289 [24] Julian Ost, Fahim Mannan, Nils Thuerey, Julian Knodt, and Felix Heide. Neural scene graphs
290 for dynamic scenes. *2021 IEEE/CVF Conference on Computer Vision and Pattern Recognition
291 (CVPR)*, pages 2855–2864, 2021.
- 292 [25] Yen-Chen Lin, Peter R. Florence, Jonathan T. Barron, Alberto Rodriguez, Phillip Isola, and
293 Tsung-Yi Lin. inerf: Inverting neural radiance fields for pose estimation. *2021 IEEE/RSJ
294 International Conference on Intelligent Robots and Systems (IROS)*, pages 1323–1330, 2021.
- 295 [26] Ricardo Martin-Brualla, Noha Radwan, Mehdi S. M. Sajjadi, Jonathan T. Barron, Alexey Dosovitskiy,
296 and Daniel Duckworth. NeRF in the Wild: Neural Radiance Fields for Unconstrained
297 Photo Collections. In *CVPR*, 2021.